Structural Analysis of Iron and Manganese Species in Iron- and Manganese-Promoted Sulfated Zirconia

Takashi Yamamoto,* Tsunehiro Tanaka,* Sakae Takenaka, and Satohiro Yoshida

Department of Molecular Engineering, Kyoto University, Kyoto 606-8501, Japan

Tsutomu Onari, Yoshiaki Takahashi, Tomomi Kosaka, and Sadao Hasegawa

Department of Chemistry, Tokyo Gakugei University, Tokyo 184-0015, Japan

Masataka Kudo

Criminal Investigation Laboratory, Metropolitan Police Department, Tokyo 100-8929, Japan

Received: November 10, 1998; In Final Form: January 26, 1999

The structural analyses of Fe, Mn−SO_4^{2-}/ZrO_2 (FMSZ), Fe−SO_4^{2-}/ZrO_2 (FSZ), Mn−SO_4^{2-}/ZrO_2 (MSZ), and Fe−Mn/ZrO_2 (FMZ) were carried out by means of XAFS, XRD, and Raman spectroscopy. Local structure around Fe and Mn of each catalyst, which were at a working state for *n*-butane isomerization and in vacuo, were studied by in situ XAFS. The valence of the Fe atom of all the catalysts was invariantly trivalent. Coordination environment around Fe of all the catalysts was quite similar to each other. Fe atoms are present inside the bulk phase of ZrO_2, the system of which forms interstitial-type solid solution and located at the center of distorted oxygen octahedra. Reaction gas does not directly make contact with Fe atoms because the introduction of reaction gas did not cause any change of coordination environment and the valence. The Mn species on FMSZ and MSZ were present as $MnSO_4$, and their coordination environment was reversibly affected by exposure to *n*-butane. Without sulfate ions, Mn species are present on the catalyst as α-Mn_2O_3.

Introduction

Since Arata et al. discovered SO_4^{2-}/ZrO_2 (SZ), which catalyzes *n*-butane skeletal isomerization at room temperature,[1] SZ and promoted SZ have been investigated extensively.[2−4] As a promoter, various transition metals have been added to SZ. In the 1990s, Hsu et al. discovered sulfated Fe−Mn−Zr oxide (FMSZ), the activity of which for *n*-butane isomerization at room temperature was higher by 3 orders of magnitude than that of conventional SO_4^{2-}/ZrO_2.[5] Furthermore, the deactivation of FMSZ for skeletal isomerization was much suppressed even in the absence of hydrogen. Therefore, much attention has been paid to this new solid acid catalyst.[6] However, the distinct difference in physical property except for catalysis between SZ and FMSZ has not been clarified.[7,8] Further, the role and structure of promoted elements on FMSZ remained unclear, in contrast to the case of Pt−SO_4^{2-}/ZrO_2.[3,9] Only a few studies were performed to investigate the states of Fe and Mn atoms on FMSZ because FMSZ contains no more than very small amounts of Fe (ca. 1.5 wt %) and Mn (ca. 0.5 wt %).

Tábora et al. measured Zr K-edge EXAFS spectrum of FMSZ and concluded that the phase of ZrO_2 was tetragonal.[10] They also measured Fe K-edge EXAFS spectrum and reported that Fe atoms were supported on ZrO_2 as small clusters or rafts of Fe_2O_3. However, its quality and the method of data reduction of the Fe K-edge EXAFS were not adequate, and it is difficult to obtain the information about the local structure around Fe. From XPS investigations, Milbum et al. reported that both Fe and Mn atoms were supported on sulfated zirconia in an oxidized state.[11] Unfortunately, their recorded X-ray photoelectron spectra of Fe_{2p}, Mn_{2p}, and S_{2s} were too noisy to determine the accurate binding energies. More recently, Gates and coworkers investigated the structure of FMSZ with various spectroscopic methods. From XPS, ESR, UV−vis, and Raman characterizations, they concluded that Fe atoms are present as small Fe_2O_3 particles with some isolated Fe^{3+} ions, and Mn atoms are present as divalent ions.[12] In contrast, Wan et al. speculated that high-valent iron oxy species such as tetrahedral Fe^{4+} species had formed on FMSZ, and these sites are responsible for the oxidative dehydrogenation of *n*-butane to butene.[13]

If Fe^{4+} species had formed on FMSZ, Fe ions would have been reduced by exposure of butane and some change of the coordination environment should have occurred. In the present study, we carried out in situ XAFS measurements to investigate the local structures around Fe and Mn atoms and studied their changes during *n*-butane isomerization.[14] There are no studies investigating coordination environment of Fe and Mn species at a working state.

Experimental Section

Material. Fe- and Mn-promoted sulfated zirconia (Fe, Mn−SO_4^{2-}/ZrO_2; FMSZ) was prepared according to Cheung's method.[15] The sulfate-ion-treated $Zr(OH)_4$ ($SO_4^{2-}/Zr(OH)_4$) was prepared by the impregnation of $Zr(OH)_4$ with 1 M $(NH_4)_2SO_4$ aqueous solution at room temperature for 0.5 h with stirring followed by filtration and drying at 383 K for 6 h. The $Zr(OH)_4$ was obtained by hydrolysis of $ZrOCl_2 \cdot 8H_2O$ with 25 mass % NH_3 aqueous solution at room temperature followed by filtration. The final value of pH was 8.0, and the aging time was 2 h. The obtained gel was washed with distilled water repeatedly until Cl^- was free on the basis of the $AgNO_3$ test. Fe and Mn ions were supported on $SO_4^{2-}/Zr(OH)_4$ by stepwise

10.1021/jp984378j CCC: $18.00
Published on Web 03/12/1999

TABLE 1: BET Specific Surface Area and Chemical Composition

catalyst	surface area $m^2\ g^{-1}$	elements (wt %)		
		S	Fe	Mn
ZrO_2	33			
SO_4^{2-}/ZrO_2	98	0.88		
Fe, Mn$-SO_4^{2-}/ZrO_2$	124	0.81	1.7	0.25
Fe$-SO_4^{2-}/ZrO_2$	107	0.96	1.1	
Mn$-SO_4^{2-}/ZrO_2$	101	1.5		0.27
Fe, Mn/ZrO_2	110		1.9	0.42

equilibrium adsorption of 0.2 M $Fe(NO_3)_3 \cdot 6H_2O$ and 0.043 M $Mn(NO_3)_2 \cdot 9H_2O$ aqueous solutions. Each equilibrium adsorption was performed at room temperature for 0.5 h with stirring followed by filtration. After drying at 383 K for 6 h, it was then calcined at 873 K for 3 h.

Fe$-SO_4^{2-}/ZrO_2$ (FSZ), Mn$-SO_4^{2-}/ZrO_2$ (MSZ), and Fe$-$Mn$/ZrO_2$ (FMZ) were prepared the same as FMSZ was prepared, by omitting each step.

Elemental composition was determined by X-ray fluorescence (XRF) with a RIGAKU 3270 spectrometer. The BET specific surface area measurement was carried out with BELSORP 28SA using a N_2 adsorption isotherm at 77 K. Results of elemental analysis and surface area measurements are summarized in Table 1.

X-ray Diffractions (XRD). X-ray diffraction patterns of samples were obtained with a RIGAKU RINT 1300 diffractometer using Ni-filtered Cu Kα radiation (averaged as 1.5418 Å).

Raman Spectra. The laser Raman spectra were recorded with a JASCO NRS-2000 spectrometer using the 514.5 nm line of an Ar^+ laser emission. An incident laser power was 0.5$-$5 mW at sample position, and the scan time was 60$-$180 s for a single spectrum. The spectral resolution was 4 cm^{-1}. All spectra were recorded under ambient conditions at room temperature.

In Situ XAFS Measurements. Fe and Mn K-edge X-ray absorption experiments were carried out on the BL7C and BL12C at Photon Factory in High Energy Accelerator Research Organization (KEK-PF; Tsukuba, Japan) with a ring energy of 2.5 GeV and a stored current of 250$-$400 mA (Proposal No. 97G041). The X-ray absorption spectra of catalysts were recorded in fluorescent mode, and those of reference compounds were recorded in transmission mode with a Si(111) two-crystal monochromator. The energy was calibrated by the preedge peak position of Cu foil (8980.3 eV).

Data reduction was performed using a FACOM M1800 computer of Kyoto University Data Processing Center. The normalization method has been previously reported in detail.[16] For curve-fitting analysis, the following EXAFS formula was applied.

$$k^3\chi(k) = \sum_j (k^2 N_j / R_j^2) A_j(k) \exp(-2\sigma_j^2 k^2) \sin(2kR_j + \delta_j(k))$$

where k is the wavenumber of the photoelectron, N_j the number of scattering atoms of the jth shell located at a distance of R_j from a central atom, A_j the envelope function that includes the backscattering amplitude and damping factor caused by inelastic loss during electron traveling, σ_j the Debye$-$Waller factor, and δ_j the phase shift. For curve-fitting analysis, the backscattering amplitude and phase shift functions of Fe$-$O pair were obtained from a k^3-weighted EXAFS spectrum of the CoO crystal (rock salt type, $a_0 = 4.260$ Å). For Zr atom scatterers, they were estimated with FEFF (6.0).[17] EXAFS analysis for Mn K-edge could not be performed because the S/N ratio of each spectrum was too bad to obtain useful information.

Each catalyst was charged in an in situ XAFS cell with a Kapton window to prevent exposure to the air. The recorded XAFS spectra of each catalyst were pretreated ones (1), ones at a working state for *n*-butane isomerization (2), and ones evacuated after a reaction (3). XAFS experiments and *n*-butane isomerization were carried out at the same time.

Catalysis. The isomerization of *n*-butane was performed with an in situ XAFS cell under static conditions at 293 K, at the same time as the XAFS measurement. The cell was made of Pyrex glass and was connected with a glass balloon filled with *n*-butane (54.1 mmol). Total dead volume of the cell was 1300 cm^3. The catalyst of FMSZ (700 mg) was evacuated at 673 K for 1 h followed by contact with *n*-butane at 293 K. After 24 h in a static condition, Fe and Mn K-edge XAFS spectra were recorded at a working state. Then reaction gases were evacuated at room temperature for 10 min followed by measurement of Fe and Mn K-edge XAFS spectra. The evacuated gas was stored in another vessel, and the composition was analyzed with TCD gas chromatography.

In the cases of FSZ, MSZ, and FMZ, XAFS measurements and *n*-butane isomerization were carried out in a manner similar to that mentioned above. For these three catalysts, another type of in situ XAFS cell, the dead volume of which was 60 cm^3, was used. The amounts of catalyst and substrate were 200 mg and 99 μmol, respectively. Catalysis over SO_4^{2-}/ZrO_2 (SZ) was performed under the same reaction conditions, using a closed reaction vessel (60 cm^3). In all cases, reaction time and temperature were 24 h and 293 K, respectively.

Results

Catalysis. After 24 h at 293 K under static conditions, 12.5% of the *n*-butane had converted to isobutane over FMSZ. The amount of reacted *n*-butane was 6.76 mmol. Formation of C_3 and C_5 species was negligible. The amounts of Fe and Mn contained in 700 mg of FMSZ were 213 and 32 μmol, respectively. The apparent turn over numbers per one Fe and Mn atoms were 32 and 211, respectively.

Over FSZ and MSZ, 25% and 7.3% of *n*-butane were converted to isobutane, respectively. The conversion over SZ was 5.8%. FMZ was inert for *n*-butane isomerization. In the case of FSZ, the amount of reacted *n*-butane was 24.8 μmol and the amount containing an Fe atom was 39 μmol. In the case of MSZ, the amount of reacted *n*-butane was 7.2 μmol and the amount containing an Mn atom was 9.8 μmol.

Because the reaction vessels for the FMSZ catalyst and for the others are different, we cannot directly compare the activity between them. But it is obvious that the activity for FMSZ is the highest. FSZ exhibited higher activity than SZ. Lange et al. observed Mn increases the activity by 2 or 3 orders of magnitude.[18] Whereas in our case, Mn addition to SZ is not very effective, the same as in the previous report.[7]

XRD. Figure 1 shows XRD patterns of catalysts calcined at 873 K. ZrO_2 consists of a mixture of monoclinic and tetragonal phases. SZ, FMSZ, and FSZ consist of only tetragonal ZrO_2 of metastable phase. The ZrO_2 phases of FMZ and MSZ are mainly tetragonal. Any peaks, other than ZrO_2 phases, were not observed in all the XRD patterns.

Raman Spectra. It has been reported that the tetragonal phase of ZrO_2 exhibits typical Raman bands at 148, 263, 325, 472, 608, and 640 cm^{-1} [19] and that the Raman spectrum of SO_4^{2-}/ZrO_2 is identical to that of tetragonal ZrO_2.[12,20,21] Raman spectra of the catalysts are shown in Figure 2. Although the XRD pattern of ZrO_2 shows that ZrO_2 consists of both monoclinic and tetragonal phases, the Raman spectrum of ZrO_2 calcined at 873

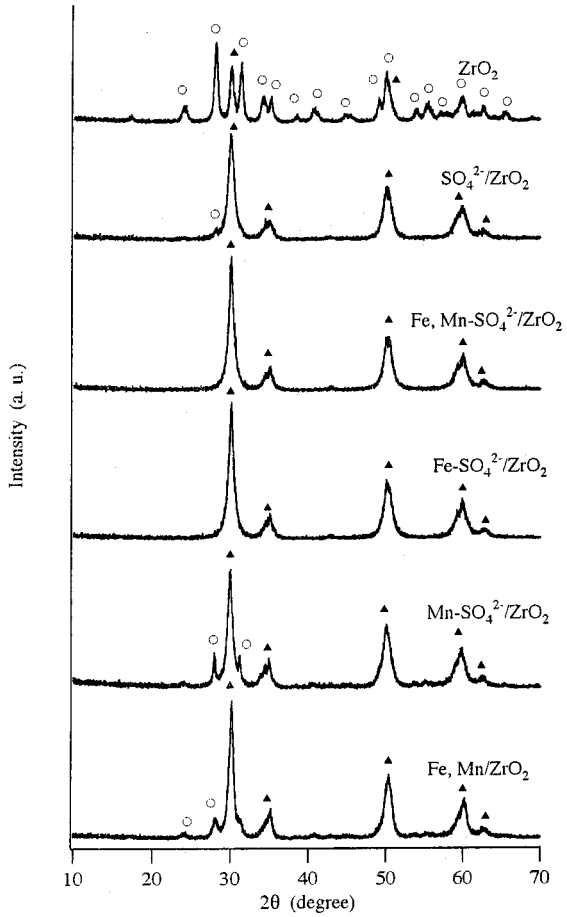

Figure 1. Cu Kα XRD patterns of samples calcined at 873 K: (○) monoclinic phase; (▲) tetragonal phase.

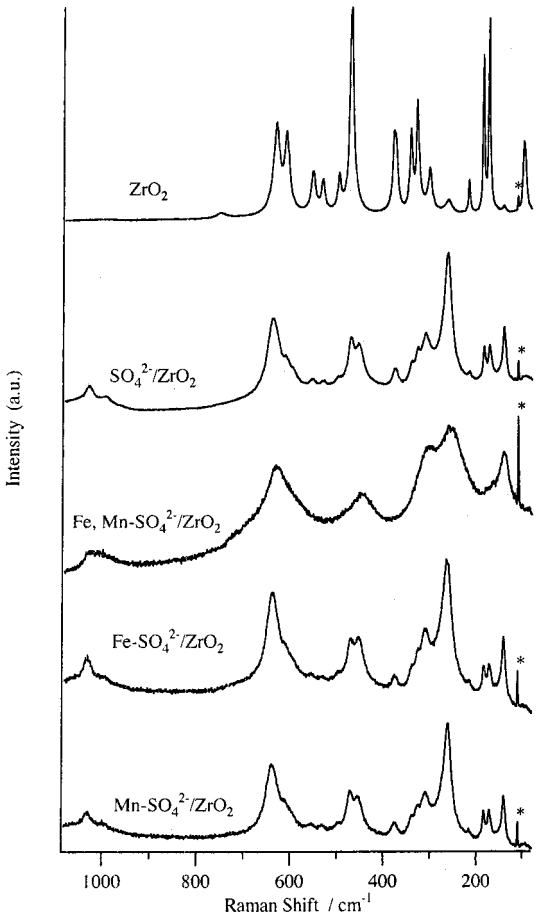

Figure 2. Raman spectra of catalysts: (*) plasma lines.

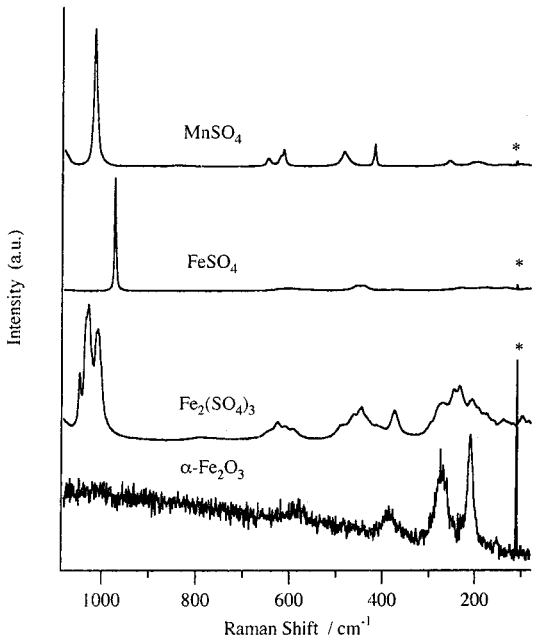

Figure 3. Raman spectra of reference compounds: (*) plasma lines.

K is identical to the reported spectrum of 100% monoclinic ZrO_2.[19] The positions of the observed Raman bands were 96, 140, 173, 185, 216, 260, 301, 328, 342, 378, 471, 499, 533, 553, 610, 632, and 752 cm^{-1}. Two tiny peaks at 140 and 260 cm^{-1} were due to the tetragonal phase, and the others were due to the monoclinic phase. It shows that the surface region of ZrO_2 calcined at 873 K consists of the monoclinic phase only, whereas the bulk is a mixture of two phases. The Raman spectrum of SZ shows that the surface phase is mainly the tetragonal ZrO_2 phase with a trace amount of monoclinic phase. The surface ZrO_2 phases of FMSZ, FSZ, and MSZ consist mainly of the tetragonal phase as well, corresponding to the results of XRD measurements. The positions of the Raman bands assigned to the tetragonal ZrO_2 phase were 140, 261, 310, 450, and 635 cm^{-1}. Scheithauer et al. measured the Raman spectra of SZ, FSZ, FMSZ, and MSZ. They confirmed that ZrO_2 phases of all the catalysts were tetragonal only, and also observed the characteristic Raman bands of α-Fe_2O_3 on the spectrum of FMSZ.[12] In contrast, we did not observe any bands due to α-Fe_2O_3 (210, 272, 386, 579 cm^{-1}) on all the spectra. α-Mn_2O_3 and β-MnO_2 exhibit no Raman bands in this region.[22]

Characteristic hydrated sulfate groups were observed on SZ, FMSZ, FSZ, and MSZ at 1029−1031 cm^{-1}, as well as Scheithauer's results. In the range of 950−1050 cm^{-1}, sulfate groups of reference compounds exhibit characteristic Raman bands at 1016 cm^{-1} for $MnSO_4$, 973 cm^{-1} for $FeSO_4$, and 1010, 1029, 1034 sh, and 1047 cm^{-1} for $Fe_2(SO_4)_3$, as shown in Figure 3. These Raman bands of metal sulfates appeared in a region similar to those of the sulfate group of SZ. In addition, Tábora et al. measured IR spectra of activated FMSZ and SZ without exposure to air.[10] In the sulfate region, IR spectra of both SZ and FMSZ exhibited strong two peaks at 1010 and 1043 cm^{-1}. Both wavenumbers are similar to those of characteristic Raman bands of $MnSO_4$ (1016 cm^{-1}) and $Fe_2(SO_4)_3$ (1010, 1028, 1047 cm^{-1}). With Raman and IR spectroscopy, it is very difficult to prove the presence of $MnSO_4$ and to determine the origin of sulfate groups of catalysts.

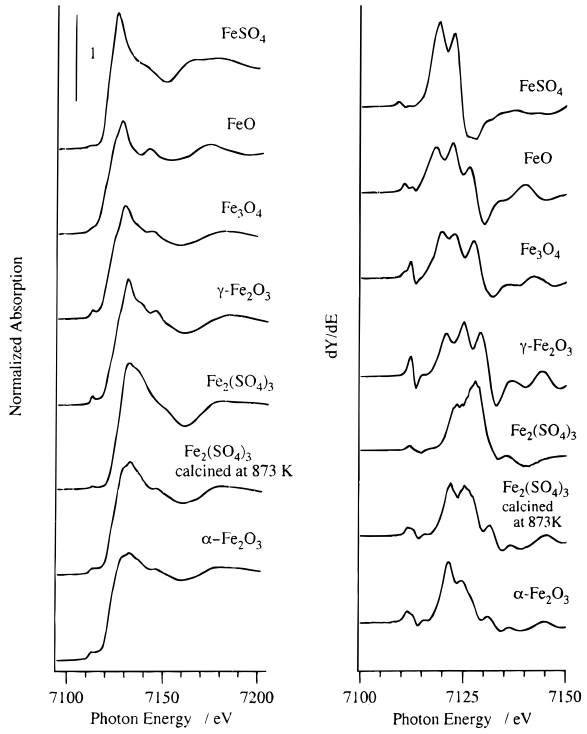

Figure 4. Fe K-edge XANES spectra of reference compounds and their first derivatives. Spectra of FeO, Fe_3O_4, γ-Fe_2O_3 were recorded on the BL10B at KEK-PF with a Si(311) channel-cut monochromator. The others were recorded on the BL7C at KEK-PF with a Si(111) two-crystal monochromator.

Fe K-Edge XANES. Figure 4 shows Fe K-edge XANES spectra and the first derivatives of reference compounds. The chemical shift between Fe^{2+} and Fe^{3+} was observed in the edge position of each spectrum. XANES spectra show that $Fe_2(SO_4)_3$ had transformed to α-Fe_2O_3 when it was calcined at 873 K. As for the Fe^{3+} species, the preedge peak of α-Fe_2O_3 was split but that of γ-Fe_2O_3 was not.

Fe K-edge XANES spectra and their first derivatives of the samples are shown in Figure 5. It is very interesting that XANES spectra of all the catalysts, including the feature and the height of preedge peaks, the edge positions, and the shapes of all spectra, were almost the same as each other. The edge energy shows that Fe atoms of the three catalysts were in the trivalent state. However, XANES spectra of all the catalysts were quite different from those of reference compounds. It shows that Fe atoms on sulfated zirconia are not present as compounds such as the reference samples shown in Figure 4. Furthermore, the local structure around Fe of all the catalysts is not affected by the presence of sulfate or Mn ions. As pointed out in the case of FMSZ previously,[14] reaction gas did not affect the edge energy or the shape of XANES spectra. Similar phenomena were observed in XANES spectra of FSZ and FMZ. Redox of Fe atoms on all the catalysts did not take place under reaction conditions. Evacuation of reacted gas did not cause any change of XANES spectra of the catalyst samples as well.

The preedge peak of Fe K-edge XANES is assigned to the 1s−3d transition, which is formally dipole-forbidden. The peak intensity is closely related to the symmetry around Fe atoms, and this peak becomes more intense as the symmetry is distorted from a regular octahedron.[23,24] Each preedge peak area of all the catalyst samples was a little larger than that of octahedral Fe^{3+} compounds such as α-Fe_2O_3 and did not change during *n*-butane isomerization. However, the preedge peak area was smaller than those of Fe−MFI and $FePO_4$, whose local structure

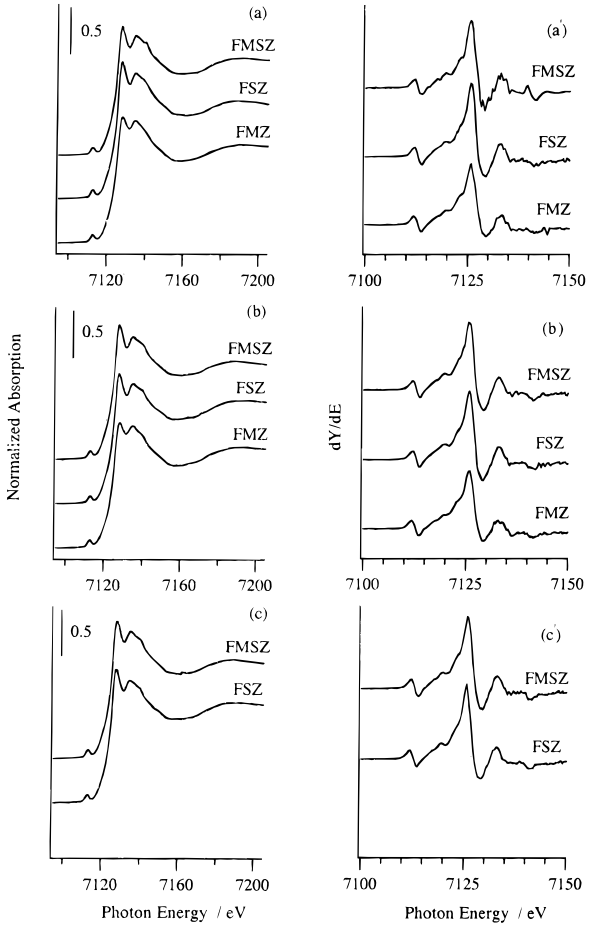

Figure 5. XANES spectra and their first derivatives of catalysts evacuated at 673 K (a), at a working state (b), and evacuated at room temperature after reaction (c).

around Fe is an FeO_4 tetrahedron.[25] It shows that the local symmetry around Fe was not tetrahedral but distorted more than that of α-Fe_2O_3. The symmetrical environment around Fe of each sample was not affected by reaction gas. In addition, the differential XANES spectrum of α-Fe_2O_3 exhibits a doublet preedge peak; however, those of FMSZ have only singlet curves. These results strongly suggest the local structure around Fe is quite different from that of α-Fe_2O_3. We propose that Fe atoms are located at a center of a highly distorted octahedron. Because the reacted amounts of *n*-butane much exceeded those of Fe atoms contained in FMSZ, it could be concluded that *n*-butane does not affect the structure or the valence of Fe as well. If any chemical reaction and/or change of coordination environment had occurred on Fe species, some changes would have been observed in XANES spectra of catalyst samples.

Mn K-Edge XANES. Figure 6 shows the Mn K-edge XANES spectra of reference compounds and their first derivatives. As previously reported,[26] the edge positions of manganese oxides shift to higher energy with increasing the oxidation number. The divalent compounds of MnO and $MnSO_4$ exhibit quite similar edge energies in XANES spectra.

Figure 7 shows the Mn K-edge XANES spectra and their first derivatives of catalyst samples. The edge positions of MSZ and FMSZ evacuated at 673 K indicate that Mn atoms were present as a divalent form. The shapes of these two XANES spectra are quite similar to that of $MnSO_4$. In contrast, the Mn K-edge XANES spectrum of FMZ exhibits the identical edge position of the trivalent. The shapes of its XANES spectrum and the first derivative resemble those of α-Mn_2O_3. Although

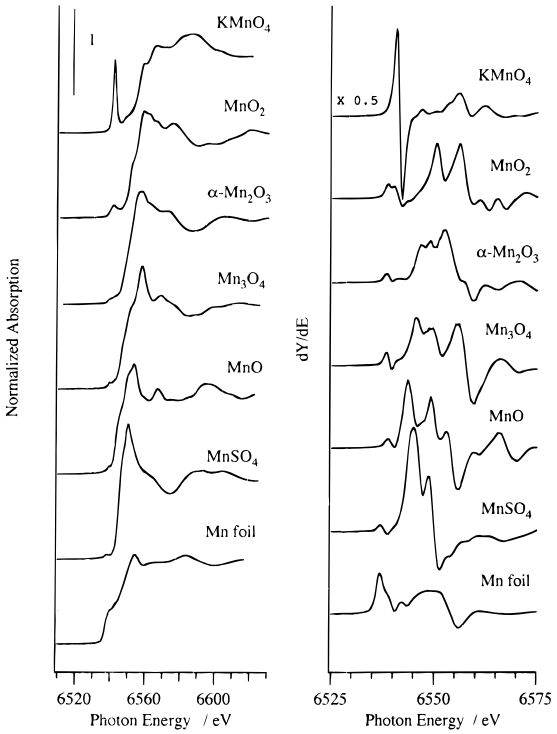

Figure 6. Mn K-edge XANES spectra and their first derivatives of reference compounds.

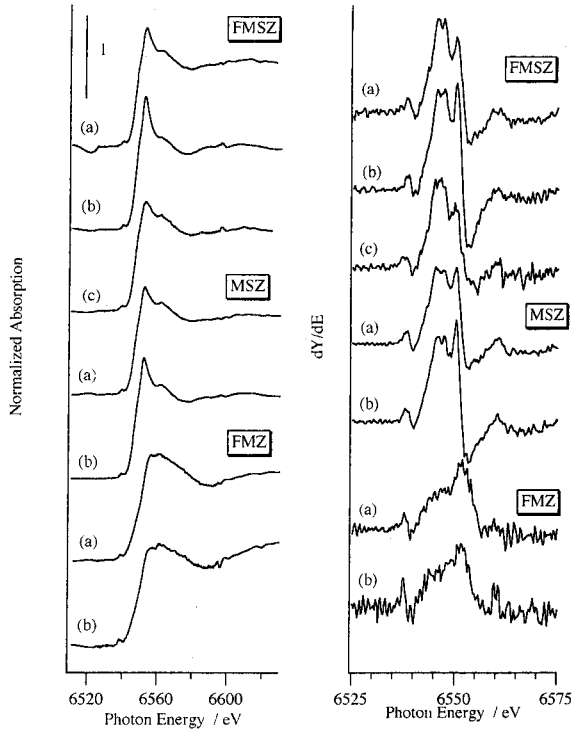

Figure 7. Mn K-edge XANES spectra and their first derivatives of catalysts evacuated at 673 K (a), at a working state (b), and evacuated at room temperature after reaction (c).

they were noisy because of the low concentration of Mn species, the similarity of XANES spectra between FMZ and α-Mn_2O_3 especially support this deduction. These results indicate that Mn atoms are present as $MnSO_4$ on sulfated ZrO_2, whereas Mn atoms are present as α-Mn_2O_3 on sulfate-free ZrO_2.

At a working state, the postedge peak of the Mn K-edge XANES of FMSZ was sharpened, but the edge position did not change. After evacuation, the shape of the postedge peak had turned back to the original state. This reversible change of XANES spectra corresponds to the change of the coordination environment around Mn. It indicates that the Mn atom is present on the surface and directly makes contacts with *n*-butane. A similar phenomenon was observed in XANES spectra of MSZ. No change was observed on those of FMZ.

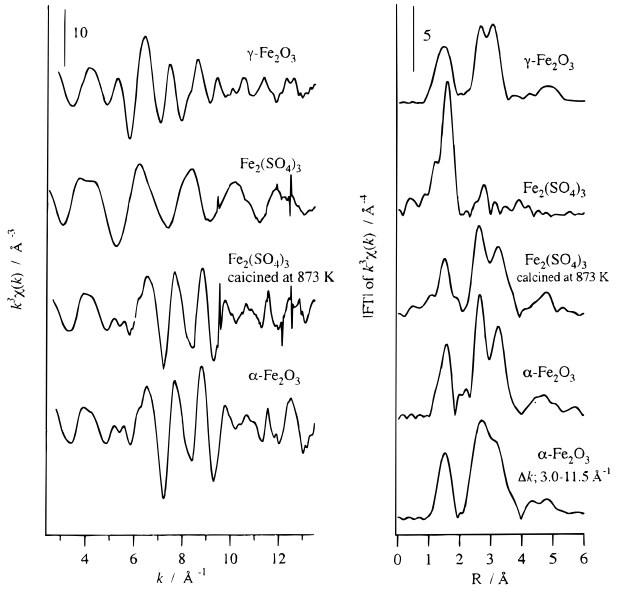

Figure 8. Fe K-edge EXAFS spectra and their Fourier transforms of reference Fe^{3+} compounds.

Fe K-Edge EXAFS. Figure 8 shows k^3-weighted Fe K-edge EXAFS spectra of Fe^{3+} reference compounds and their Fourier transforms in the *k*-range of 3−14 $Å^{-1}$. An EXAFS spectrum of $Fe_2(SO_4)_3$ calcined at 873 K and its Fourier transform are identical to those of α-Fe_2O_3. Even if supported Fe species on sulfated zirconia had formed $Fe_2(SO_4)_3$, it might be decomposed in the calcination step at 873 K.

Figure 9 shows k^3-weighted Fe K-edge EXAFS spectra of the catalyst samples. EXAFS spectra of FMSZ, FSZ, and FMZ, which were pretreated, are similar to each other. All spectra of the catalyst samples are quite different from those of reference compounds. Although *S*/*N* ratios of EXAFS spectra are not good, we conclude that the three EXAFS spectra of the catalyst samples are identical. These results suggest that short-range structure around Fe was not affected by any additives such as manganese and/or sulfate ions. In the case of FMSZ, the three variously treated EXAFS spectra are also quite similar to each other. It clearly shows that the short-range structure of FMSZ around Fe was not affected by *n*-butane at all. The exposure to *n*-butane also did not affect the local structure of FSZ and FMZ around Fe as well.

Figure 10 shows Fourier transforms of Fe K-edge k^3-weighted EXAFS spectra of the catalyst samples. Because the noise level of each spectrum is different, Fourier filtered ranges of EXAFS spectra are not regular. The transformed ranges of pretreated FMSZs and the other two spectra are 3−13 and 3−14 $Å^{-1}$, respectively. The ranges of all FSZs are 3−11.5 $Å^{-1}$. Those of pretreated FMZs and their working states are 3−11.5 and 3−10 $Å^{-1}$, respectively. In all of their radial structure functions (RSFs) except for that of FMZ at the working state, two distinct peaks appeared around 1.6 and 3.3 Å. The peak around 1.6 Å is due to oxygen scatterers. The position of the peak around 3.3 Å is higher than those of α-Fe_2O_3 and γ-Fe_2O_3, which are due to Fe atoms. Therefore, we assigned the second peak due to scattering not from Fe but from Zr atoms. In contrast to our results, Tábora et al. did not observe the second peak in the

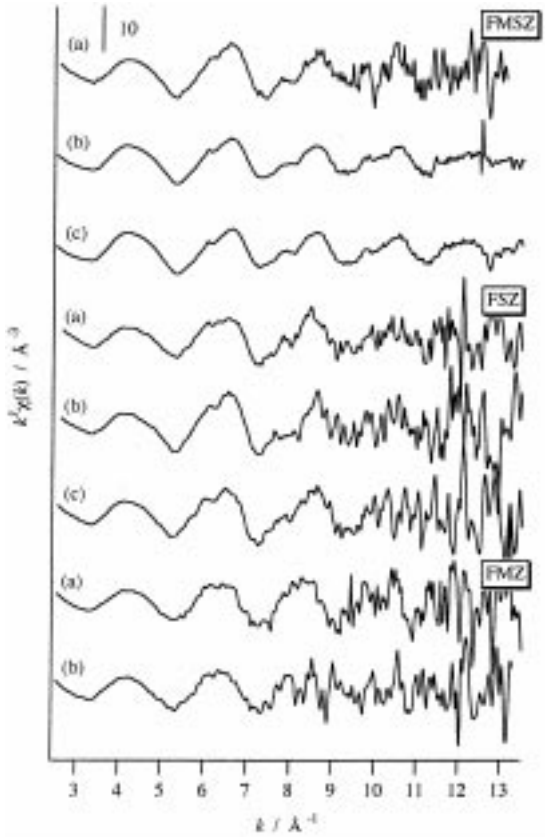

Figure 9. Fe K-edge EXAFS spectra of catalysts evacuated at 673 K (a), at a working state (b), and evacuated at room temperature after reaction (c).

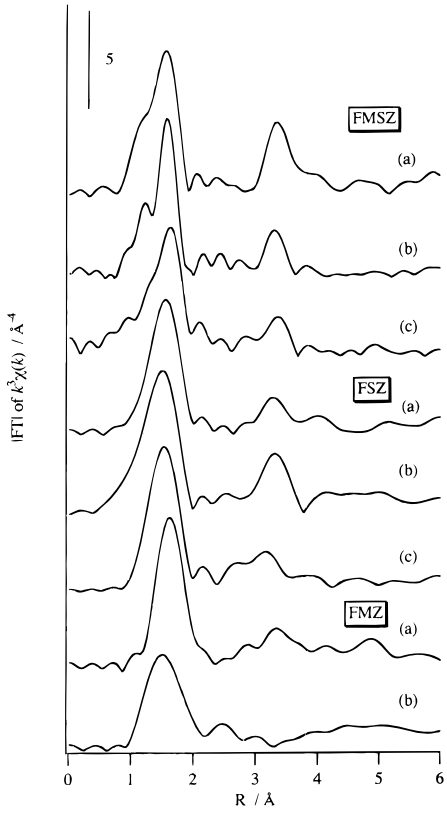

Figure 10. Fourier transforms for k^3-weighted Fe K-edge EXAFS of catalysts evacuated at 673 K (a), at a working state (b), and evacuated at room temperature after reaction (c).

RSF of FMSZ.[10] The reason for the difference between our results and their work is the data reduction of EXAFS spectra. In the case of Tábora's work, it seems that the subtracted background was not adequate, especially over $k = 7$ Å^{-1}. In addition, they adopted k^2-weighted EXAFS, in contrast to our k^3-weighted EXAFS spectra.

To obtain further information, we performed curve-fitting analysis. The results are summarized in Table 2. As examples, the fits of Fourier filtered Fe K-edge EXAFS for pretreated and at a working state of FMSZ are shown in Figure 11. The first coordination spheres for all the catalysts could not be fit with a single Fe−O shell but could be fit with two shells. Only that of pretreated FMZs gave a satisfactory fit with a single shell. For the first shell of all the catalyst samples, each estimated parameter is identical within calculation errors. Their interatomic distances and coordination numbers are similar to those of α-Fe_2O_3, the coordination environment of which is 6-fold.[27] An Fe atom of α-Fe_2O_3 is surrounded by six oxygen atoms, but the interatomic distances are not uniform. The bond lengths of three Fe−O pairs are ca. 1.91 Å, and those of three more Fe−O pairs are ca. 2.06 Å.[28] The estimated EXAFS parameter strongly suggests that Fe species in all the catalyst samples are present at the center of oxygen octahedron. An estimated coordination number for the first shell of pretreated FMZ is 4.6; however, the interatomic distance is 2.02 Å. For 4-fold coordination materials, the bond length between Fe and O atoms has been reported to be 1.85 Å for Fe−MFI[25] and $FePO_4$ [29] and to be 1.89 Å for Fe/Na−SiO_2.[30] The estimated distance (2.02 Å) of the Fe−O bond in pretreated FMZ is much longer than those for 4-fold coordination. Therefore, we conclude that the Fe species on pretreated FMZ is also in 6-fold coordination. From the fact that each height of the preedge peak of the catalysts is higher than those of $Fe_2(SO_4)_3$ and α-Fe_2O_3, the FeO_6 octahedra of catalyst samples are supposed to be distorted.

TABLE 2: Results of Curve-Fitting Analysis

sample	shell	CN[a]	R/Å[b]	$\Delta\sigma^2$/Å^2 [c]
Fe, Mn−SO_4^{2-}/ZrO_2 pretreated	Fe-O	3.0	1.86	−0.0048
		2.9	1.99	−0.0075
	Fe−Zr	1.5	3.62	0.0037
under reaction	Fe-O	3.0	1.85	−0.0021
		3.0	1.98	−0.0062
	Fe−Zr	1.5	3.60	0.0070
after evacuation	Fe-O	2.8	1.88	−0.0035
		2.8	2.01	−0.0064
	Fe−Zr	1.9	3.61	0.0090
Fe−SO_4^{2-}/ZrO_2 pretreated	Fe−O	2.6	1.91	−0.0067
		2.6	2.03	−0.0069
	Fe−Zr	3.1	3.58	0.0127
under reaction	Fe-O	2.9	1.87	−0.0085
		2.9	2.00	−0.0090
	Fe−Zr	4.1	3.60	0.0110
after evacuation	Fe-O	2.8	1.90	−0.0081
		2.9	2.03	−0.0084
	Fe−Zr	4.3	3.53	0.0140
Fe, Mn/ZrO_2 pretreated	Fe-O	4.6	2.02	−0.0037
	Fe−Zr	1.1	3.62	0.0051
under reaction	Fe-O	2.9	1.91	−0.0065
		2.9	2.07	−0.0066
	Fe−Zr			
α-Fe_2O_3[d]	Fe-O	3.0	1.91	0.0007
		2.9	2.04	0.0023

[a] Coordination number. [b] Interatomic distance. [c] Debye−Waller factor. [d] Taken from ref 27.

The peaks around 3.3 Å observed in RSFs of samples could be assigned to scatterers from Zr atoms, as shown in Table 2. The estimated interatomic distances are almost the same as each

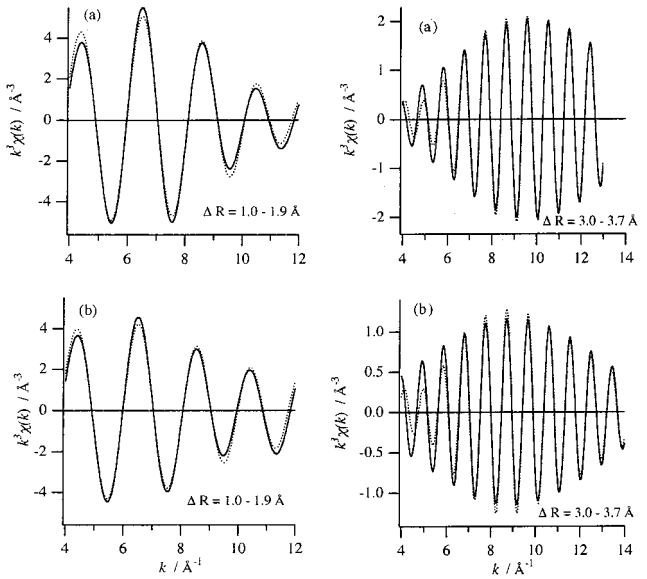

Figure 11. Fits of Fourier-filtered EXAFS of FMSZ: pretreated (a, a′); working state (b, b′). The solid curves were obtained experimentally, and the dotted ones were the fits.

other (3.60 ± 0.02 Å). These bond lengths are close to the Zr−Zr bonding of tetragonal ZrO_2,[31] ZS, and FMSZ.[10] In our analysis, the estimated coordination number ranged from 1.1 to 4.1. However, we recognize that the estimated coordination number is not very important. Because the noise level of the higher *k*-region of many spectra is not sufficient, the reliability of the absolute value seems not to be high. The important points are the facts that contributions from Zr were observed and that the coordination number was much smaller than 12. The reason will be discussed in the following section. A lack of the second peak in RSF of FMZ of the working state is due to the low quality of its EXAFS spectrum, not really to the lack of contribution from the second neighbors.

Discussion

Structure around Fe. XRD patterns indicate that ZrO_2 phases of all promoted catalysts are tetragonal. The phase of sulfated zirconia calcined at 873 K is reported by many researchers as tetragonal by XRD,[2,3] Raman,[12,20,21] and EXAFS characterizations.[10] In our analysis, the ZrO_2 phase of sulfate-ion-free FMZ was also tetragonal. XRD analysis suggests that iron and/or manganese atoms also affect the crystal phase of ZrO_2 to form the tetragonal metastable phase as well as sulfate ions. The similar effects were observed in WO_3-ZrO_2 and MoO_3-ZrO_2 systems.[2] According to the phase diagram for Fe−Zr−O system, Fe_2O_3 forms a solid solution with ZrO_2 when the content of Fe oxide is up to a few mol %.[32] In the case of FMSZ, an Fe fraction as Fe_2O_3 is 1.85 mol % for ZrO_2. That for FMZ is 2.08 mol %. These concentrations permit formation of a solid solution. Therefore, we conclude that Fe and Zr oxide of all the catalyst samples formed solid solutions. Because the ion radius of Fe^{3+} (0.67 Å) is much smaller than that of Zr^{4+} (0.87 Å), the type of solid solution is supposed to be interstitial, not substitutional. If Fe_2O_3 and ZrO_2 formed substitutional-type solid solution, Fe atom would be in 8-fold coordination and the coordination number for the Fe−Zr shell should be estimated to be 12. In fact, the Y K-edge EXAFS analysis of 3 mol % $Y_2O_3-ZrO_2$ revealed that the estimated coordination number for the Y−O and Y−Zr shells were 8 and 12, respectively.[31b,c] In addition, the Zr−O bond length of tetragonal ZrO_2 is 2.260 ± 0.208 Å, the coordination number of which is 8, and that for monoclinic ZrO_2 is 2.160 ± 0.085 Å, the coordination number of which is 7.[31a] If the Fe atom was in 7- or 8-fold coordination, the Fe−O bond length is expected to be much longer than that of α-Fe_2O_3 of 6-fold coordination. In our analysis, however, coordination numbers for the Fe−Zr shell of all the samples were much smaller than 12, and the bond lengths for Fe−O shells were close to those for α-Fe_2O_3. These coordination numbers for Fe−Zr pairs and the bond length for Fe−O pairs support the deduction that the type of solid solution is interstitial and that Fe atoms are present inside the bulk of ZrO_2. Both sulfate and/or manganese ions, which are present on the surface of catalysts, did not affect the coordination environment around Fe. It is consistent with the fact that the local structure around Fe was not affected by the exposure to *n*-butane.

Formation of Solid Solution. XAFS studies of Fe−Zr−O systems have been performed by Berthet et al.[33] and Ji et al.[34] Berthet et al. prepared a cubic solid solution of $Zr_{0.70}Fe_{0.30}O_{1.85}$ by calcination of the coprecipitates of hydroxides. They observed two peaks around 1.4 and 3 Å in the RSF of the Fe K-edge EXAFS and assigned the second peak to the Fe−Zr shell. They reported that the coordination number and interatomic distance for the second shell were 4.1 and 3.29 Å, respectively. This bond length was much shorter than those of our results (3.60 Å). In their work, the molar fraction of Fe_2O_3 was 18 mol %, which remarkably exceeds the limit of solid solution formation. At that fraction, a mixture of ZrO_2 solid solution and hematite solid solution will be formed, as shown in the phase diagram.[32] Therefore, the second peak they observed around 3 Å in the RSF might not be due to Zr scatterers, but to Fe scatterers.

Ji et al. prepared Fe/ZrO_2 by equilibrium adsorption of Fe ions onto ZrO_2, in which the loading amount of Fe was 0.5 wt %, followed by calcination at 773 K.[34] They observed the second peak in the RSF of Fe K-edge EXAFS around 2.6 Å and concluded that the second peak was due to Fe−Fe scatterers, the coordination number and interatomic distance of which were 1.1 and 3.11 Å, respectively.

In Ji's study, the concentration of Fe is possible to form a solid solution with ZrO_2; however, the solid solution was not formed. The difference between our result and Ji's study results from the preparation methods. For the support of Fe species, Li et al. used the ZrO_2 crystal (16 $m^2\ g^{-1}$).[35] In our study, iron was supported onto $Zr(OH)_4$ (391 $m^2\ g^{-1}$) or $SO_4^{2-}/Zr(OH)_4$. We believe that the definitive difference is whether the support was ZrO_2 or $Zr(OH)_4$. In the calcination step, Fe/$Zr(OH)_4$ or Fe−SO_4^{2-}/$Zr(OH)_4$ had transformed to Fe/ZrO_2 or Fe−SO_4^{2-}/ZrO_2 with formation of solid solutions. In the case of Ji's study, it seems to be difficult for Fe atoms to form a solid solution with the ZrO_2 crystal. It was supported by the results that two kinds of 7 mol % Fe_2O_3/ZrO_2 catalysts, which were prepared by the impregnation method onto the ZrO_2 crystal and the coprecipitation method, exhibit a remarkable difference in catalytic property for CO hydrogenation and reducibility of Fe atoms.[36]

Structure of Manganese Species. We have reported that the Mn atom was supported on the surface of FMSZ as $MnSO_4$.[14] From an ESR study, Scheithauer et al. concluded that Mn^{2+} atoms were supported on MSZ and FMSZ in a highly dispersed form, although their structures remained unknown.[12] In the present study, Mn K-edge XANES spectra revealed that the Mn species on MSZ and FMSZ are present as $MnSO_4$. The calcination temperature of each sample was 873 K, which is lower than the decomposition temperature of $MnSO_4$. The decomposition temperature of $MnSO_4$ is 1123 K, while that of

$Fe_2(SO_4)_3$ is 753 K.[37] Therefore, the assumption that $MnSO_4$ was present on the catalysts is adequate.

In contrast to the cases of FMSZ and MSZ, manganese species on FMZ were identified as α-Mn_2O_3. It was reported that α-Mn_2O_3 and α-Mn_3O_4 are formed by calcination of manganese salt under air at 873 and 1073 K, respectively.[22] Because the sulfate ion was free and the calcination temperature of the precursor was 873 K, α-Mn_2O_3 was formed on FMZ. In addition, MnO_2 polymorphism might be formed if the precursor of FMZ was calcined at lower than 773 K.

Role of Fe and Mn Ion. Wan et al. speculated that a high-valent iron oxy species such as the tetrahedral Fe^{4+} species have formed during calcination in air, and the site is responsible for the oxidative dehydrogenation of *n*-butane to produce butenes.[13] However, our present XANES analysis indicates that the Fe atom on each catalyst sample was invariantly trivalent. Although the reacted amounts of *n*-butane much exceeded those of Fe atoms contained in the catalyst, it is obvious that reduction of the Fe atom did not occur during reaction. Tábora stated that Fe atoms in FMSZ are not substituted isomorphously into bulk tetragonal ZrO_2 but instead are in nanometer-size oxide clusters or rafts located on the surfaces or at defects in tetragonal ZrO_2.[10] Scheithauer et al. concluded from ESR analysis that small Fe_2O_3 particles are present in FSZ and FMSZ, with some isolated Fe^{3+} ions.[12] In contrast to their opinions, we conclude that Fe^{3+} ions of FMSZ, FSZ, and FMZ are present inside the bulk of tetragonal ZrO_2 to form interstitial-type solid solutions, and each Fe atom is isolated from other Fe atoms. The formation of the Fe_2O_3 particle may depend on the preparation method. As discussed above, Fe atoms of all the catalyst samples are present inside the bulk phases and do not make contact with the reactant gas. It shows that the Fe atom does not directly participate in *n*-butane skeletal isomerization. Nevertheless, not only FMSZ but also FSZ exhibit quite higher activity for the isomerization than SZ. We speculate that the role of Fe ions is to influence somewhat the surface energy level of SO_4^{2-}/ZrO_2, although we do not have any evidence for it.

It is well-known that many metal sulfates exhibit solid acidity.[38,39] However, these metal sulfates merely exhibit moderate acid strength, the maximum of which are $H_0 = -3$. It is impossible to catalyze *n*-butane isomerization at around 300 K over these kinds of acid sites. This is supported by the result of catalysis that MSZ exhibited only activity similar to that of SZ. However, local structures around Mn on FMSZ and MSZ were affected by the presence of *n*-butane, as shown in XANES spectra. Therefore, it can be concluded that Mn sites on FMSZ are not active sites. Because the coordination environment around Mn was affected by the introduction of reactant gas, we propose that the role of the Mn site on Fe, $Mn-SO_4^{2-}/ZrO_2$ would be to accelerate transformation of reactants to active sites on SO_4^{2-}/ZrO_2. The rapid transformation of substrates results in a remarkable enhancement of the catalytic activity. The combination of two different kinds of promoters enhances remarkably the catalytic activity of SZ.

Arata et al. reported that iron oxide treated with sulfate ion exhibited solid superacidity and catalyzed *n*-butane isomerization even at 273 K.[2,40] However, in the present case of Fe, $Mn-SO_4^{2-}/ZrO_2$, the so-called SO_4^{2-}/Fe_2O_3 was not formed.

Conclusion

Fe oxide and Zr oxide forms interstitial-type solid solutions, regardless of the presence of sulfate and/or Mn ions. The local structures around Fe atoms in Fe, $Mn-SO_4^{2-}/ZrO_2$, $Fe-SO_4^{2-}/ZrO_2$, and Fe, Mn/ZrO_2 are quite similar to each other. Fe atoms of all the catalysts are trivalent and located at the center of oxygen octahedron. The Fe atom is present inside the bulk of ZrO_2, and the local structure and the valence were not influenced by *n*-butane. Mn atoms are present as $MnSO_4$ on the surface of sulfated zirconia and as α-Mn_2O_3 on unsulfated zirconia. Under reaction conditions, *n*-butane molecules make contact with Mn atoms and are desorbed by evacuation.

Acknowledgment. We are indebted to Professor M. Nomura (KEK-PF) for carrying out the X-ray measurements. This work was partially supported by a Grant-in-Aid (No. 08405052) from Japan Ministry of Education, Science, Sports, and Culture.

References and Notes

(1) Hino, M.; Kobayashi, S.; Arata, K. *J. Am. Chem. Soc.* **1979**, *101*, 6439.
(2) Arata, K. *Adv. Catal.* **1990**, *37*, 165.
(3) Song, X.; Sayari, A. *Catal. Rev. Sci. Eng.* **1996**, *38*, 329.
(4) Corma, A.; Gacía, H. *Catal. Today* **1997**, *38*, 257.
(5) Hsu, C.-Y.; Heimbuch, C. R.; Armes, C. T.; Gates, B. C. *J. Chem. Soc., Chem. Commun.* **1992**, 1645.
(6) Cheung, T.-K.; Gates, B. C. *Top. Catal.* **1998**, *6*, 41 and references therein.
(7) Jatia, A.; Chang, C.; MacLeod, J. D.; Okubo, T.; Davis, M. E. *Catal. Lett.* **1994**, *25*, 21.
(8) Adeeva, V.; de Haan, J. W.; Jänchen, J.; Lei, G. D.; Schünemann, V.; van de Ven, L. J. M.; Sachatler, W. M. H.; van Santen, A. *J. Catal.* **1995**, *151*, 364.
(9) Hattori, H.; Shishido, T. *Catal. Survey Jpn.* **1997**, *1*, 205.
(10) Tábora, J. E.; Davis, R. J. *J. Chem. Soc., Faraday Trans.* **1995**, *91*, 1825.
(11) Milbum, D. R.; Keogh, R. A.; Sparks, D. E.; Davis, B. H. *Appl. Surf. Sci.* **1998**, *126*, 11.
(12) Scheithauer, M.; Bosch, E.; Schubert, U.; Knözinger, H.; Cheung, T.-K.; Jentoft, F. C.; Gates, B. C.; Tesche, B. *J. Catal.* **1998**, *177*, 137.
(13) Wan, K. T.; Knou, C. B.; Davis, M. E. *J. Catal.* **1996**, *158*, 311.
(14) Yamamoto, T.; Tanaka, T.; Takenaka, S.; Yoshida, S.; Onari, T.; Takahashi, Y.; Kosaka, T.; Hasegawa, S. *J. Synchrotron Radiat.*, in press.
(15) Cheung, T.-K.; d'Itri, J. L.; Gates, B. C. *J. Catal.* **1995**, *151*, 464.
(16) Tanaka, T.; Yamashita, H.; Tsuchitani, R.; Funabiki, T.; Yoshida, S. *J. Chem. Soc., Faraday Trans. 1* **1988**, *84*, 2987.
(17) Rehr, J. J.; Mustre de Leon, J.; Zabinsky, S. I.; Albers, R. C. *J. Am. Chem. Soc.* **1991**, *113*, 5135.
(18) Lange, F. C.; Cheung, T.-K.; Gates, B. C. *Catal. Lett.* **1996**, *41*, 95.
(19) Mercera, P. D. L.; van Ommen, J. G.; Doesburg, E. B. M.; Burggraaf, A. J.; Ross, J. R. H. *Appl. Catal.* **1990**, *57*, 127.
(20) Spielbauer, D.; Mekhemer, G. A. H.; Bosch, E.; Knözinger, H. *Catal. Lett.* **1996**, *36*, 59.
(21) Li, C.; Stair, P. C. *Catal. Lett.* **1996**, *36*, 119.
(22) Strohmeisr, B. R.; Herules, D. M. *J. Phys. Chem.* **1984**, *88*, 4922.
(23) Bart, J. C. J. *Adv. Catal.* **1986**, *34*, 203.
(24) Westre, T. E.; Kennepohl, P.; DeWitt, J. G.; Hedman, B.; Hodgson, K. O.; Solomon, E. I. *J. Am. Chem. Soc.* **1997**, *119*, 6297.
(25) Bordiga, S.; Buzzoni, R.; Geobaldo, F.; Lamberti, C.; Giamello, E.; Zecchina, A.; Leofanti, G.; Petrini, G.; Tozzola, G.; Vlaic, G. *J. Catal.* **1996**, *158*, 486.
(26) Brown, N. M. D.; McMonagle, J. B.; Greaves, G. N. *J. Chem. Soc., Faraday Trans. 1* **1984**, *80*, 589.
(27) Kanai, H.; Mizutani, H.; Tanaka, T.; Funabiki, T.; Yoshida, S.; Takano, M. *J. Mater. Chem.* **1992**, *2*, 703.
(28) Wyckoff, R. W. G. *Crystal Structures*, 2nd ed.; Interscience Publishers: New York, 1986; Vol. 2, pp 6−8.
(29) Goiffon, A. *Rev. Chim. Miner.* **1986**, *23*, 99.
(30) Zhang, H.; Niu, J.-Z.; Kou, Y.; Tanaka, T.; Yoshida, S. *J. Solid State Chem.* **1998**, *137*, 325.
(31) (a) Li, P.; Chen, I.-W.; Penner-Hahn, J. E. *Phys. Rev. B* **1993**, *48*, 10063. (b) Li, P.; Chen, I.-W.; Penner-Hahn, J. E. *Phys. Rev. B* **1993**, *48*, 10074. (c) Li, P.; Chen, I.-W.; Penner-Hahn, J. E. *Phys. Rev. B* **1993**, *48*, 10082.
(32) Jones, T. S.; Kimura, S.; Muan, A. *J. Am. Ceram. Soc.* **1967**, *50*, 137.
(33) Berthet, P.; Berthon, J.; Revcolevschi, A. *Physica B* **1989**, *158*, 506.
(34) Ji, W.; Kou, Y.; Shen, S.; Li, S.; Wang, H. *Proc. Int. Congr. Catal., 10th* **1993**, 2060.

(35) Ji, W.; Shen, S.; Li, S.; Wang, H. *Stud. Surf. Sci. Catal.* **1991**, *63*, 517.
(36) Chen, K.; Fan, Y.; Hu, Z.; Yan, Q. *Catal. Lett.* **1996**, *36*, 139.
(37) Kubo, R., Nagakura, S., Iguchi, Y., Ezawa, H., Eds. *Iwanami Rikagaku-Jiten*, 4th ed.; Iwanami-Shoten: Tokyo, 1987 (in Japanese).
(38) Tanabe, K. *Solid Acids and Bases*; Kodansha: Tokyo, 1970; pp 80−89.
(39) Tanabe, K.; Misono, M.; Ono, Y.; Hattori, H. *New Solid Acids and Bases*; Kodansha: Tokyo, 1989; pp 185−188.
(40) Hino, M.; Arata, K. *Chem. Lett.* **1979**, 1259.